Nonlinear Adaptive Control for Electromagnetic Actuators

Benosman, M.; Atinc, G.M.

TR2015-024 January 19, 2015

Abstract

The authors study here the problem of adaptive "soft-landing" control for electromagnetic actuators. The soft landing requires accurate control of the actuator's moving element between two desired positions. They propose a non-linear adaptive controller to solve the problem of robust trajectory tracking for the moving element, when considering model uncertainties with linear parametrisation. The controller is an integral input-to-state stability (iISS) backstepping controller, merged with gradient descent estimation filters to estimate model uncertainties with linear parametrisation. They show that it ensures bounded tracking errors for bounded estimation errors. Furthermore, iISS result allows us to represent the bound on tracking error as a decreasing function of the estimation error. They demonstrate the effectiveness of this controller with numerical tests.

IET Control Theory & Applications

Nonlinear Adaptive Control for Electromagnetic Actuators

Mouhacine Benosman
Mitsubishi Electric Research Laboratories
201 Broadway Street, Cambridge, MA 02139, USA
Gökhan M. Atınç
Mechanical Science and Engineering Department
University of Illinois at Urbana-Champaign, USA

Abstract

We study here the problem of adaptive 'soft-landing' control for electromagnetic actuators. The soft landing requires accurate control of the actuator's moving element between two desired positions. We propose a nonlinear adaptive controller to solve the problem of robust trajectory tracking for the moving element, when considering model uncertainties with linear parametrization. The controller is an integral Input-to-State Stability (iISS) backstepping controller, merged with gradient descent estimation filters to estimate model uncertainties with linear parametrization. We show that it ensures bounded tracking errors for bounded estimation errors. Furthermore, iISS result allows us to represent the bound on tracking error as a decreasing function of the estimation error. We demonstrate the effectiveness of this controller with numerical tests.

I. Introduction

Nowadays, electromagnetic actuators are used in many practical applications, e.g. opening and closing cargo doors in aircraft systems, precision positioning stages actuation, brakes in industrial systems. In this work we concentrate on a particular control problem of nonlinear electromagnetic actuator called 'soft landing' problem. The soft landing requires accurate control of the moving element of the actuator between two desired positions. This 'soft-landing' performance has to be guaranteed over long periods of time during which the actuator components may age. The main objective is to attain small contact velocity, which in turn ensures low component-wear operation of the actuator. Due to these practical constraints we have developed a robust control algorithm that aims for a zero impact velocity, and adapts to some of the actuator aging parts. We present here the results of this study.

Many papers have been dedicated to the soft-landing problem for electromagnetic actuators, e.g. [1]-[10]. Several controllers have been developed in [1], [4], [5], [9] based on linear models of the system. Linear models allow for a relatively easy design of the control but due to their linearity, are not valid for a full operation range of the actuator. To control the system over a larger operating state space, the controller has to be based on more complex nonlinear models of the actuators. Different nonlinear controllers have been used in [2], [3], [6], [8], [11], [12], [10], [13]. For example in [6], the authors proposed a nonlinear controller to solve the problem of armature stabilization for an electromechanical valve actuator. The authors proved

Corresponding author: M. Benosman (benosman@merl.com)

a global asymptotic stability result using Sontag's nonlinear controller. However, this approach did not solve the problem of armature trajectory tracking and did not consider robustness of the controller with respect to system's uncertainties and changes in parameters over time. In [2], the authors studied the problem of electromagnetic valve actuator control in an internal combustion engine. The solution proposed by the author is based on iteratively solving a constrained nonlinear optimal problem using Nelder-Mead algorithm. The robustness of this feedforward-based approach has neither been proven nor tested. In [12], the authors designed a backstepping based controller for electromagnetic actuators position regulation. However, robustness w.r.t. uncertainties in parameters of the system are not considered in this paper. In [10], the authors designd a feasible trajectory within the solenoid voltage limits, and then used a flatness-based controller designed on a nominal model, i.e. without model uncertainties, to track the desired trajectory. In [13], a Lyapunov-based controller was designed to stabilize the armature in finite time. The controller was tuned using numerical analysis. This controller can be considered as a passive robust control designed to compensate for bounded friction forces. In [8], a nonlinear sliding mode approach was used to solve the problem of trajectory tracking for an electromagnetic valve actuator. The authors used a nonlinear model to design the sliding mode control. The reported results showed good tracking performances, however, the sliding mode controller uses discontinuous control signals to ensure the convergence to a sliding surface, which could over-stress the actuator. Furthermore, sliding-mode control is well known to be a passive robust controller, in the sense that it deals with model uncertainties with a pre-defined range of uncertainties, which might necessitate higher control amplitude than what is actually needed, and could be unable to cope with uncertainties that falls outside of the expected uncertainties' bounds. In [3], the authors used a single parameter extremum seeking learning method to solve the problem of soft landing for an electromechanical valve actuator. In [14], a multiparameter extremum seeking-based control was presented. The authors first designed a nonlinear controller based on Lyapunov redesign technique and then added a multiparameter extremum seeking algorithm to tune the feedback gains of the controller. Although the learning algorithms in [3], [14] were not directly tailored to ensure robustness of the controller with respect to model uncertainties or parameters drift over time, one could argue that this robustness is intrinsic due the iterative nature of the learning process. In [15], the authors designed a backstepping based controller for electromagnetic actuators which was robustified by an extremum seeking algorithm to estimation some uncertain parameters of the system. The effectiveness of the proposed scheme was illustrated numerically, however, no rigorous analysis was present concerning the stability of the combined model-based nominal controller and the model-free learning algorithm.
In this work, we propose an alternative solution to the robust soft-landing problem. We choose an active robust control approach, and use a nonlinear model of the electromagnetic actuator to design a nonlinear adaptive backstepping controller. We use the so-called integral Input-to-State stability (iISS) theory to develop a nonlinear iISS-adaptive controller, merged with gradient-descent estimation filters. This controller ensures bounded tracking errors as well as bounded estimation errors. Furthermore, due to the iISS result, we can show that the tracking errors decrease with the estimation errors.

This paper is organized as follows: We first present in Section II some notations and preliminaries. In Section III, we recall the nonlinear model of electromagnetic actuators. Then, in Section IV, we report the adaptive nonlinear controller, with stability analysis. Numerical validation of the proposed controller is given in Section V, and finally, concluding remarks are stated in Section VI.

II. Preliminaries

Throughout the paper we use the notation $\dot{(.)}$ for the short notation of time derivative, and we use $\|.\|$ to denote the Euclidean norm; i.e., for $x \in \mathbb{R}^n$ we have $\|x\| = \sqrt{x^T x}$. Also, we denote by C^k functions that are k times differentiable. A continuous function $\alpha : [0, a) \to [0, \infty)$ is said to belong to class $\mathcal{K}$ if it is strictly increasing and $\alpha(0) = 0$. It is said to belong to class $\mathcal{K}_\infty$ if $a = \infty$ and $\alpha(r) \to \infty$ as $r \to \infty$. A continuous function $\beta : [0, a) \times [0, \infty) \to [0, \infty)$ is said to belong to class $\mathcal{KL}$ if, for each fixed s, the mapping $\beta(r, s)$ belongs to class $\mathcal{K}$ with respect to r and, for each fixed r, the mapping $\beta(r, s)$ is decreasing with respect to s and $\beta(r, s) \to 0$ as $s \to \infty$.

Next, we introduce some definitions that will be used in the paper. To help present the definitions in a general setting, we first consider the general dynamical time-varying system

$$\dot{x}(t) = f(t, x(t)), \quad x(t_0) = x_0, \quad t \geq t_0 \tag{1}$$

where $x(t) \in \mathcal{D} \subseteq \mathbb{R}^n$ such that $0 \in \mathcal{D}$, $f : [t_0, t_1) \times \mathcal{D} \to \mathbb{R}^n$ is such that $f(\cdot, \cdot)$ is jointly continuous in t and x, and for every $t \in [t_0, t_1)$, $f(t, 0) = 0$ and $f(t, \cdot)$ is locally Lipschitz in x uniformly in t for all t in compact subsets of $[0, \infty)$. The above assumptions guarantee the existence and uniqueness of the solution $x(t)$ over the interval $[t_0, t_1)$. Without loss of generality, we assume $t_0 = 0$.

Definition 1 (LaSalle-Yoshizawa [16]): Consider the time-varying system (1) and assume $[0, \infty) \times \mathcal{D}$ is a positively invariant set with respect to (1) where $f(t, \cdot)$ is Lipschitz in x, uniformly in t. Assume there exist a C^1 function $V : [0, \infty) \times \mathcal{D} \to \mathbb{R}$, continuous positive definite functions $W_1(\cdot)$ and $W_2(\cdot)$ and a continuous nonnegative function $W(\cdot)$, such that for all $(t, x) \in [0, \infty) \times \mathcal{D}$,

$$\begin{aligned} W_1(x) \leq V(t, x) \leq W_2(x), \\ \dot{V}(t, x) \leq -W(x) \end{aligned} \tag{2}$$

Then, there exists $\mathcal{D}_0 \subseteq \mathcal{D}$ such that for all $(t_0, x_0) \in [0, \infty) \times \mathcal{D}_0$, $x(t) \to \mathcal{R} \triangleq \{x \in \mathcal{D} : W(x) = 0\}$ as $t \to \infty$. If, in addition, $\mathcal{D} = \mathbb{R}^n$ and $W_1(\cdot)$ is radially unbounded, then for all $(t_0, x_0) \in [0, \infty) \times \mathbb{R}^n$, $x(t) \to \mathcal{R} \triangleq \{x \in \mathbb{R}^n : W(x) = 0\}$ as $t \to \infty$.

Definition 2 (Integral Input-to-State Stability [17]): Consider the system

$$\dot{x} = f(t, x, u) \tag{3}$$

where $x \in \mathcal{D} \subseteq \mathbb{R}^n$ such that $0 \in \mathcal{D}$,and $f : [0, \infty) \times \mathcal{D} \times \mathcal{D}_u \to \mathbb{R}^n$ is piecewise continuous in t and locally Lipschitz in x and u, uniformly in t. The inputs are assumed to be measurable and locally essentially bounded functions $u : \mathbb{R}_{\geq 0} \to \mathcal{D}_u \subseteq \mathbb{R}^m$. Given any control $u \in \mathcal{D}_u$ and any $\xi \in \mathcal{D}_0 \subseteq \mathcal{D}$, there is a unique maximal solution of the initial value problem $\dot{x} = f(t, x, u)$, $x(t_0) = \xi$. Without loss of generality, assume $t_0 = 0$. The unique solution is defined on some maximal open interval, and it is denoted by $x(\cdot, \xi, u)$. System (3) is locally integral input-to-state stable (LiISS) if there exist functions α, $\gamma \in \mathcal{K}$ and $\beta \in \mathcal{KL}$ such that, for all $\xi \in \mathcal{D}_0$ and all $u \in \mathcal{D}_u$, the solution $x(t, \xi, u)$ is defined for all $t \geq 0$ and

$$\alpha(\|x(t, \xi, u)\|) \leq \beta(\|\xi\|, t) + \int_0^t \gamma(\|u(s)\|) ds \tag{4}$$

for all $t \geq 0$. Equivalently, system (3) is LiISS if and only if there exist functions $\beta \in \mathcal{KL}$ and γ_1, $\gamma_2 \in \mathcal{K}$ such that

$$\|x(t, \xi, u)\| \leq \beta(\|\xi\|, t) + \gamma_1 \left(\int_0^t \gamma_2(\|u(s)\|) ds \right) \tag{5}$$

for all $t \geq 0$, all $\xi \in \mathcal{D}_0$ and all $u \in \mathcal{D}_u$.

Definition 3 (iISS-Lyapunov [18],[19]): A C^1 function $V : \mathcal{D} \to \mathbb{R}$ is called an iISS-Lyapunov function for system (3) if there exist functions α_1, α_2, $\sigma \in \mathcal{K}$, and a continuous positive definite function α_3, such that

$$\alpha_1(\|x\|) \leq V(t,x) \leq \alpha_2(\|x\|) \tag{6}$$

for all $x \in \mathcal{D}$ and

$$\dot{V} \leq -\alpha_3(\|x\|) + \sigma(\|u\|) \tag{7}$$

for all $x \in \mathcal{D}$ and all $u \in \mathcal{D}_u$.

Definition 4 (Smooth Dissipativity [19]): System (3) with output h is dissipative if there exists a C^1, proper and positive definite function V, together with a $\sigma \in \mathcal{K}$ and a continuous positive definite function α_4, such that

$$\dot{V} \leq -\alpha_4(\|h(x(t,\xi,u))\|) + \sigma(\|u\|) \tag{8}$$

for all $x \in \mathcal{D}$ and all $u \in \mathcal{D}_u$. If this property holds with a V that is also smooth, system (3) with output h is said to be *smoothly dissipative*. Finally, if (8) holds with $h = 0$, i.e., there exists a smooth proper and positive definite V, and a $\sigma \in \mathcal{K}$, so that

$$\dot{V} \leq \sigma(\|u\|) \tag{9}$$

holds for all $x \in \mathcal{D}$ and all $u \in \mathcal{D}_u$, the system (3) is said to be *zero-output smoothly dissipative*.

Definition 5 (Weakly Zero-Detectability [19]): Let an output for the system (3) be a continuous map $h : \mathcal{D} \to \mathbb{R}^p$, with $h(0) = 0$. For each initial state $\xi \in \mathcal{D}_0$, and each input $u \in \mathcal{D}_u$, let $y(t,\xi,u)$ be the corresponding output function; i.e., $y(t,\xi,u) = h(x(t,\xi,u))$, defined on some maximal interval $[0, T_{\xi,u})$. The system (3) with output h is said to be *weakly zero-detectable* if, for each ξ such that $T_{\xi,0} = \infty$ and $y(t,\xi,0) \equiv 0$, it must be the case that $x(t,\xi,0) \to 0$ as $t \to \infty$.

Definition 6 (0-input locally uniformly asymptotically stable [20]): The system (3) is 0-input locally uniformly asymptotically stable (0-LUAS), if the unforced system

$$\dot{x} = f(t,x,0) \tag{10}$$

is LUAS.

We are now ready to present our work on the specific type of systems studied here, namely, electromagnetic actuators. We first recall a well known nonlinear model of this system.

III. System modelling

Following e.g., [3], [11], we consider the nonlinear electromagnetic actuator model

$$\begin{aligned} m\frac{d^2x}{dt^2} &= k(x_0 - x) - \eta\frac{dx}{dt} - \frac{ai^2}{2(b+x)^2} + f_d \\ u &= Ri + \frac{a}{b+x}\frac{di}{dt} - \frac{ai}{(b+x)^2}\frac{dx}{dt},\ 0 \leq x \leq x_f, \end{aligned} \tag{11}$$

where, x represents the armature position physically constrained between the initial position of the armature 0, and the maximal position of the armature x_f, $\frac{dx}{dt}$ represents the armature velocity, m is the armature mass, k the spring constant, x_0 is the initial length of the spring, η is the damping coefficient (assumed to be constant), $\frac{ai^2}{2(b+x)^2}$ represents the electromagnetic force (EMF) generated by the coil, a, b being constant parameters of the coil, f_d a constant term modelling disturbance forces, e.g. static friction, R the resistance of the coil, $L = \frac{a}{b+x}$ the coil inductance (assumed to be armature-position dependent), $\frac{ai}{(b+x)^2}\frac{dx}{dt}$ represents the back EMF. Finally, i denotes the coil current, $\frac{di}{dt}$ its time derivative and u represents the control voltage applied to the coil.

IV. Adaptive Nonlinear Backstepping Control

A. iISS Adaptive Backstepping Controller

Consider the dynamical system (11), and let us define the state vector $\mathbf{z} := [z_1 \quad z_2 \quad z_3]^T = [x \quad \dot{x} \quad i]^T$. The objective of the control is to make the variables (z_1, z_2) track a sufficiently smooth (at least C^2) time-varying position and velocity trajectories $z_1^{ref}(t),\ z_2^{ref}(t) = \frac{dz_1^{ref}(t)}{dt}$ that satisfy the following constraints:

$$\begin{aligned} &z_1^{ref}(t_0) = z_{1_{int}}, \quad z_1^{ref}(t_f) = z_{1_f}, \\ &\dot{z}_1^{ref}(t_0) = \dot{z}_1^{ref}(t_f) = 0, \\ &\ddot{z}_1^{ref}(t_0) = \ddot{z}_1^{ref}(t_f) = 0 \end{aligned} \tag{12}$$

where t_0 is the starting time of the trajectory, t_f is the ending time, $z_{1_{int}}$ is the initial position and z_{1_f} is the final position. We want to design a controller that achieves the tracking objective in the presence of model parametric uncertainties, which makes the problem more challenging.

Let us first write the system (11) in the following way:

$$\begin{aligned} \dot{z}_1 &= z_2 \\ \dot{z}_2 &= \tfrac{k}{m}(x_0 - z_1) - \tfrac{\eta}{m} z_2 - \tfrac{a}{2m(b+z_1)^2} z_3^2 + \tfrac{f_d}{m} \\ \dot{z}_3 &= -\tfrac{R}{\frac{a}{b+z_1}} z_3 + \tfrac{z_3}{b+z_1} z_2 + \tfrac{u}{\frac{a}{b+z_1}} \end{aligned} \tag{13}$$

Consider the system in (13) with constant uncertainty in the spring constant k, the damping coefficient η and the additive disturbance f_d. Since the parameters are unknown, we will use the certainty equivalence principle [21] and define (obtained via the constructive proof of Lemma 1) the control input u where the parameters $k,\ \eta,\ f_d$ are replaced by their estimates $\hat{k}$, $\hat{\eta}$ and $\hat{f}_d$:

$$\begin{aligned} u = &\tfrac{a}{b+z_1}\Big(\tfrac{R(b+z_1)}{a} z_3 - \tfrac{z_2 z_3}{(b+z_1)} + \tfrac{1}{2z_3}\Big(\tfrac{a}{2m(b+z_1)^2}(z_2 - z_2^{ref}) - c_2(z_3^2 - \tilde{u})\Big)\Big) \\ &+ \tfrac{2mz_2}{z_3}\Big(\tfrac{\hat{k}}{m}(x_0 - z_1) + \tfrac{\hat{\eta}}{m} z_2 + \tfrac{\hat{f}_d}{m} + c_3(z_1 - z_1^{ref}) + c_1(z_2 - z_2^{ref}) + \kappa_1(z_2 - z_2^{ref})\|\psi\|_2^2 - \dot{z}_2^{ref}\Big) \\ &+ \tfrac{m(b+z_1)}{z_3}\Big(\Big(\tfrac{\hat{k}}{m}(x_0 - z_1) + \tfrac{\hat{\eta}}{m} z_2 + \tfrac{\hat{f}_d}{m} - \tfrac{a}{2m(b+z_1)^2} z_3^2 - \dot{z}_2^{ref}\Big)\Big(c_1 + \kappa_1\|\psi\|_2^2 + \tfrac{\hat{\eta}}{m}\Big) + \tfrac{\hat{\eta}}{m}\dot{z}_2^{ref}\Big) \\ &+ \tfrac{m(b+z_1)}{z_3}\Big(2\kappa_1(z_2 - z_2^{ref})\Big(\tfrac{(x_0-z_1)(-z_2)}{m^2} + \tfrac{z_2\left(\frac{\hat{k}}{m}(x_0-z_1) + \frac{\hat{\eta}}{m} z_2 + \frac{\hat{f}_d}{m} - \frac{a z_3^2}{2m(b+z_1)^2}\right)}{m^2}\Big)\Big) \\ &-\kappa_2(z_3^2 - \tilde{u})\Big|\tfrac{2m(b+z_1)^2}{a}\Big|^2\Big[\Big|c_1 + \kappa_1\|\psi\|_2^2 + \tfrac{\hat{\eta}}{m}\Big|^2 + \Big|2\kappa_1(z_2 - z_2^{ref})\Big|^2\Big|\tfrac{z_2}{m^2}\Big|^2\Big]\|\psi\|_2^2 \\ &-\kappa_3(z_3^2 - \tilde{u})\Big|\tfrac{2m(b+z_1)^2}{a}\Big|^2\|\psi\|_2^2 + \tfrac{m(b+z_1)}{z_3}\Big(-\tfrac{\hat{k}}{m} z_2 - \ddot{z}_2^{ref} + c_3(z_2 - z_2^{ref})\Big) \end{aligned} \tag{14}$$

with

$$\begin{aligned} \tilde{u} = &\tfrac{2m(b+z_1)^2}{a}\Big(\tfrac{\hat{k}}{m}(x_0 - z_1) + \tfrac{\hat{\eta}}{m} z_2 + \tfrac{\hat{f}_d}{m} + c_3(z_1 - z_1^{ref}) + c_1(z_2 - z_2^{ref}) - \dot{z}_2^{ref}\Big) \\ &+ \tfrac{2m(b+z_1)^2}{a}\Big(\kappa_1(z_2 - z_2^{ref})\|\psi\|_2^2\Big) \end{aligned} \tag{15}$$

where $\psi \triangleq \begin{bmatrix} \frac{x_0 - z_1}{m} & -\frac{z_2}{m} & \frac{1}{m} \end{bmatrix}^T$.

We can now state the following lemma.

Lemma 1: Consider the closed-loop dynamics given by (13), (14) and (15), with constant but unknown parameters k, η, f_d and the parameter error vector $\Delta \triangleq \begin{bmatrix} k - \hat{k} & \eta - \hat{\eta} & f_d - \hat{f}_d \end{bmatrix}^T$. Then, there exist positive gains c_1, c_2, c_3, κ_1, κ_2 and κ_3 such that $(z_1(t), z_2(t))$ are uniformly bounded and the system (13) is locally integral input-to state stable (LiISS) with respect to $(\Delta, \dot{\Delta})$.

Proof: Consider the mechanical subsystem that consists of only the first two equations of (13) with the virtual control input $\tilde{u} := z_3^2$:

$$\begin{aligned} \dot{z}_1 &= z_2 \\ \dot{z}_2 &= \tfrac{k}{m}(x_0 - z_1) - \tfrac{\eta}{m} z_2 + \tfrac{f_d}{m} - \tfrac{a}{2m(b+z_1)^2}\tilde{u} \end{aligned} \tag{16}$$

Defining the Lyapunov function $V_{sub} = \frac{c_3}{2}(z_1 - z_1^{ref})^2 + \frac{1}{2}(z_2 - z_2^{ref})^2$, with $c_3 > 0$, we would like to design $\tilde{u}$ so that $\dot{V}_{sub} = -c_1(z_2 - z_2^{ref})^2$ along the trajectories of (16), but since the system parameters k, η and f_d are unknown, we design the virtual input to be $\tilde{u}$ given by (15). Inserting $\tilde{u}$ from (15) into $\dot{V}_{sub}$, we obtain

$$\begin{aligned} \dot{V}_{sub} &= c_3(z_1 - z_1^{ref})(\dot{z}_1 - \dot{z}_1^{ref}) + (z_2 - z_2^{ref})(\dot{z}_2 - \dot{z}_2^{ref}) \\ &= (z_2 - z_2^{ref})(c_3(z_1 - z_1^{ref}) + \tfrac{k}{m}(x_0 - z_1) - \tfrac{\eta}{m} z_2 - \dot{z}_2^{ref} - \tfrac{a}{2m(b+z_1)^2}\tilde{u}) \\ &= -c_1(z_2 - z_2^{ref})^2 + (z_2 - z_2^{ref})(\tfrac{(k-\hat{k})(x_0-z_1)}{m} - \tfrac{(\eta-\hat{\eta})z_2}{m} + \tfrac{f_d - \hat{f}_d}{m}) - \kappa_1(z_2 - z_2^{ref})^2\|\psi\|_2^2 \end{aligned} \tag{17}$$

Using the definitions of the vectors ψ and Δ, we have

$$\begin{aligned} \dot{V}_{sub} &\le c_1(z_2 - z_2^{ref})^2 + |z_2 - z_2^{ref}|\|\psi^T\|_2\|\Delta\|_2 - \kappa_1(z_2 - z_2^{ref})^2\|\psi\|_2^2 \\ &\le -c_1(z_2 - z_2^{ref})^2 - \kappa_1\left[|z_2 - z_2^{ref}|\|\psi\|_2 - \tfrac{\|\Delta\|_2}{2\kappa_1}\right]^2 + \tfrac{\|\Delta\|_2^2}{4\kappa_1} \\ &\le -c_1(z_2 - z_2^{ref})^2 + \tfrac{\|\Delta\|_2^2}{4\kappa_1} \end{aligned} \tag{18}$$

where $\Delta = \begin{bmatrix} k - \hat{k} & \eta - \hat{\eta} & f_d - \hat{f}_d \end{bmatrix}^T$ is the vector holding the discrepancy between actual system parameters and estimated parameters. Note that we have made use of the nonlinear damping term $-\kappa_1(z_2 - z_2^{ref})^2\|\psi\|_2^2$ to attain a negative quadratic term of ψ and Δ $\left(\text{i.e.,} -\kappa_1\left[|z_2 - z_2^{ref}|\|\psi\|_2 - \frac{\|\Delta\|_2}{2\kappa_1}\right]^2\right)$ and a positive term that is a function of Δ only $\left(\frac{\|\Delta\|_2^2}{4\kappa_1}\right)$. Next, we define the Lyapunov function for the full system: $V_{aug} = V_{sub} + \frac{(z_3^2 - \tilde{u})^2}{2}$. Taking the derivative of V_{aug} along the trajectories of the full system, leads to the following inequality:

$$\begin{aligned} \dot{V}_{aug} \le& -c_1(z_2 - z_2^{ref})^2 + \tfrac{\|\Delta\|_2^2}{4\kappa_1} + (z_3^2 - \tilde{u})\left(-\tfrac{a(z_2 - z_2^{ref})}{2m(b+z_1)^2} - \dot{\tilde{u}}\right) \\ &+ (z_3^2 - \tilde{u})(2z_3(-\tfrac{R(b+z_1)}{a} z_3 + \tfrac{z_2 z_3}{(b+z_1)} + \tfrac{b+z_1}{a} u)) \end{aligned} \tag{19}$$

where $\dot{\tilde{u}}$ writes as

$$\begin{aligned} \dot{\tilde{u}} =& \tfrac{4m(b+z_1)z_2}{a}(\tfrac{\hat{k}}{m}(x_0 - z_1) - \tfrac{\hat{\eta}}{m} z_2 + \tfrac{\hat{f}_d}{m} + c_3(z_1 - z_1^{ref}) \\ &+ c_1(z_2 - z_2^{ref})) + \tfrac{4m(b+z_1)z_2}{a}(\kappa_1(z_2 - z_2^{ref})\|\psi\|_2^2 - \dot{z}_2^{ref}) \\ &+ \tfrac{2m(b+z_1)^2}{a}(\tfrac{\dot{\hat{k}}}{m}(x_0 - z_1) - \tfrac{\dot{\hat{\eta}}}{m} z_2 + \tfrac{\dot{\hat{f}}_d}{m}) + \tfrac{2m(b+z_1)^2}{a}((\tfrac{k}{m}(x_0 - z_1) \\ &- \tfrac{\eta}{m} z_2 + \tfrac{f_d}{m} - \tfrac{a}{2m(b+z_1)^2} z_3^2 - \dot{z}_2^{ref})(c_1 + \kappa_1\|\psi\|_2^2 - \tfrac{\hat{\eta}}{m}) - \tfrac{\hat{\eta}}{m}\dot{z}_2^{ref}) \\ &+ \tfrac{2m(b+z_1)^2}{a}(2\kappa_1(z_2 - z_2^{ref})(\tfrac{(x_0 - z_1) - z_2}{m^2} \\ &+ \tfrac{z_2(\frac{k}{m}(x_0 - z_1) - \frac{\eta}{m} z_2 + \frac{f_d}{m} - \frac{a z_3^2}{2m(b+z_1)^2})}{m^2})) \\ &+ \tfrac{2m(b+z_1)^2}{a}(-\tfrac{\hat{k}}{m} z_2 - \ddot{z}_2^{ref} + c_3(z_2 - z_2^{ref})) \end{aligned} \tag{20}$$

By substituting the control input given in (14) into (19), we attain the following inequality:

$$\begin{aligned} \dot{V}_{aug} \le& -c_1(z_2 - z_2^{ref})^2 + \tfrac{\|\Delta\|_2^2}{4\kappa_1} - c_2(z_3^2 - \tilde{u})^2 \\ &- (z_3^2 - \tilde{u})\left(\tfrac{2m(b+z_1)^2}{a}\left(\tfrac{(k-\hat{k})(x_0-z_1)}{m} + \tfrac{(\eta-\hat{\eta})z_2}{m} + \tfrac{f_d - \hat{f}_d}{m}\right)\left(c_1 + \kappa_1\|\psi\|_2^2 + \tfrac{\hat{\eta}}{m}\right)\right) \\ &- (z_3^2 - \tilde{u})\left(2\kappa_1(z_2 - z_2^{ref})\left(\tfrac{2z_2(b+z_1)^2}{ma}\right)\left(\tfrac{(k-\hat{k})(x_0-z_1)}{m} + \tfrac{(\eta-\hat{\eta})z_2}{m} + \tfrac{f_d - \hat{f}_d}{m}\right)\right) \\ &- (z_3^2 - \tilde{u})\left(\tfrac{2m(b+z_1)^2}{a}\right)\left(\tfrac{\dot{\hat{k}}}{m}(x_0 - z_1) + \tfrac{\dot{\hat{\eta}}}{m} z_2 + \tfrac{\dot{\hat{f}}_d}{m}\right) \\ &- \kappa_3(z_3^2 - \tilde{u})^2\left|\tfrac{2m(b+z_1)^2}{a}\right|^2\|\psi\|_2^2 \\ &- \kappa_2(z_3^2 - \tilde{u})^2\left[\left|\tfrac{2m(b+z_1)^2}{a}\right|^2\left|c_1 + \kappa_1\|\psi\|_2^2 + \tfrac{\hat{\eta}}{m}\right|^2 + \left|2\kappa_1(z_2 - z_2^{ref})\right|^2\left|\tfrac{2z_2(b+z_1)^2}{ma}\right|^2\right]\|\psi\|_2^2 \end{aligned} \tag{21}$$

Using the aforementioned definitions of the vectors ψ and Δ, and noting that $\dot{\Delta} = \begin{bmatrix} -\dot{\hat{k}} & -\dot{\hat{\eta}} & -\dot{\hat{f}}_d \end{bmatrix}^T$, we can further bound $\dot{V}_{aug}$ in the following way:

$$\begin{aligned}
&\dot{V}_{aug} \leq -c_1(z_2 - z_2^{ref})^2 + \tfrac{\|\Delta\|_2^2}{4\kappa_1} - c_2(z_3^2 - \tilde{u})^2 \\
&+\left|z_3^2 - \tilde{u}\right|\left|\tfrac{2m(b+z_1)^2}{a}\right|\left|c_1 + \kappa_1\|\psi\|_2^2 + \tfrac{\hat{\eta}}{m}\right|\|\psi^T\|_2\|\Delta\|_2 \\
&+\left|z_3^2 - \tilde{u}\right|\left|2\kappa_1(z_2 - z_2^{ref})\right|\left|\tfrac{2z_2(b+z_1)^2}{ma}\right|\|\psi^T\|_2\|\Delta\|_2 \\
&+\left|z_3^2 - \tilde{u}\right|\left|\tfrac{2m(b+z_1)^2}{a}\right|\|\psi^T\|_2\|\dot{\Delta}\|_2 \\
&-\kappa_3(z_3^2 - \tilde{u})^2\left|\tfrac{2m(b+z_1)^2}{a}\right|^2\|\psi\|_2^2 \\
&-\kappa_2(z_3^2 - \tilde{u})^2\left[\left|\tfrac{2m(b+z_1)^2}{a}\right|^2\left|c_1 + \kappa_1\|\psi\|_2^2 + \tfrac{\hat{\eta}}{m}\right|^2 + \left|2\kappa_1(z_2 - z_2^{ref})\right|^2\left|\tfrac{2z_2(b+z_1)^2}{ma}\right|^2\right]\|\psi\|_2^2
\end{aligned} \tag{22}$$

By making use of the nonlinear damping terms the same way as they have been utilized in deriving (18), we obtain

$$\begin{aligned}
&\dot{V}_{aug} \leq -c_1(z_2 - z_2^{ref})^2 + \tfrac{\|\Delta\|_2^2}{4\kappa_1} - c_2(z_3^2 - \tilde{u})^2 \\
&-\kappa_2\left[\left|z_3^2 - \tilde{u}\right|\left|\tfrac{2m(b+z_1)^2}{a}\right|\left|c_1 + \kappa_1\|\psi\|_2^2 + \tfrac{\hat{\eta}}{m}\right|\|\psi\|_2 - \tfrac{\|\Delta\|_2}{2\kappa_2}\right]^2 + \tfrac{\|\Delta\|_2^2}{4\kappa_2} \\
&-\kappa_2\left[\left|z_3^2 - \tilde{u}\right|\left|2\kappa_1(z_2 - z_2^{ref})\right|\left|\tfrac{2z_2(b+z_1)^2}{ma}\right|\|\psi\|_2 - \tfrac{\|\Delta\|_2}{2\kappa_2}\right]^2 + \tfrac{\|\Delta\|_2^2}{4\kappa_2} \\
&-\kappa_3\left[\left|z_3^2 - \tilde{u}\right|\left|\tfrac{2m(b+z_1)^2}{a}\right|\|\psi\|_2 - \tfrac{\|\dot{\Delta}\|_2}{2\kappa_3}\right]^2 + \tfrac{\|\dot{\Delta}\|_2^2}{4\kappa_3}
\end{aligned} \tag{23}$$

Finally, using the inequality (23), we have

$$\dot{V}_{aug} \leq -c_1(z_2 - z_2^{ref})^2 - c_2(z_3^2 - \tilde{u})^2 + \left(\tfrac{1}{4\kappa_1} + \tfrac{1}{2\kappa_2}\right)\|\Delta\|_2^2 + \tfrac{\|\dot{\Delta}\|_2^2}{2\kappa_3} \tag{24}$$

It is easy to see that the uncertain system can be expressed in the following nonlinear time-varying form:

$$\dot{e} = f(t, e, \tilde{\Delta}) \tag{25}$$

with $e \in \mathcal{D}_e$, $\tilde{\Delta} \in \mathcal{D}_{\tilde{\Delta}}$, where $e := [z_1 - z_1^{ref} \quad z_2 - z_2^{ref} \quad z_3^2 - \tilde{u}]^T$ and $\tilde{\Delta} = [\Delta \ \dot{\Delta}]^T$. Then, by considering the output map defined by $h = [z_2 - z_2^{ref} \quad z_3^2 - \tilde{u}]^T$, we can show by analyzing the zero-dynamics of (25) with $h \equiv 0$, $\tilde{\Delta} \equiv 0$, that the system (25) with h is weakly zero-detectable. Indeed, $\tilde{\Delta} \equiv 0$ means that we are analyzing the zero dynamics of the feedback system in the nominal case. Now considering the output condition $h \equiv 0$, together with the dynamics (15), and (16), leads to the following zero dynamics

$$\begin{aligned}
\dot{z}_1 &= z_2 \\
\dot{z}_2 &= \dot{z}_2^{ref} - c_3(z_1 - z_1^{ref}) - c_1(z_2 - z_2^{ref})
\end{aligned} \tag{26}$$

Writing the second equation in (26) in terms of z_1 and z_1^{ref} only, and introducing $e_{z_1} := z_1 - z_1^{ref}$, we obtain

$$\ddot{e}_{z_1} + c_1\dot{e}_{z_1} + c_3 e_{z_1} = 0 \tag{27}$$

It can be seen that if c_3 and c_1 are selected such that

$$-c_1 \pm \sqrt{c_1^2 - 4c_3} < 0 \tag{28}$$

the roots of the characteristic equation of (27) would be negative, which in turn would imply $\lim_{t\to\infty} z_1 = z_1^{ref}$ starting from any initial condition $z_1(t_0)$.

Next, using the weakly-zero- detectability property together with inequality (24), we can conclude that the system (25) is LiISS with respect to the input $\tilde{\Delta}$. To do so, we proceed as follows:

First, inequality (24), with $\tilde{\Delta} = 0$, leads to

$$\dot{V}_{aug} \leq -c_1(z_2 - z_2^{ref})^2 - c_2(z_3^2 - \tilde{u})^2 \tag{29}$$

which by LaSalle-Yoshizawa Theorem (Definition 1), implies that the states of the error dynamics (25) converge asymptotically to the set $\{e \in \mathcal{D}_e,\ s.t.\ h(e) = 0\}$, which by the zero-dynamics analysis presented above implies that $e \to 0$ asymptotically. This proves the 0-LUAS of the error dynamics (25). Next, using (24), we can write

$$\begin{aligned} \dot{V}_{aug} &\leq -c_1(z_2 - z_2^{ref})^2 - c_2(z_3^2 - \tilde{u})^2 + \left(\tfrac{1}{4\kappa_1} + \tfrac{1}{2\kappa_2}\right)\|\Delta\|_2^2 + \tfrac{\|\dot{\Delta}\|_2^2}{2\kappa_3} \\ &\leq \left(\tfrac{1}{4\kappa_1} + \tfrac{1}{2\kappa_2}\right)\|\Delta\|_2^2 + \tfrac{\|\dot{\Delta}\|_2^2}{2\kappa_3} \end{aligned} \tag{30}$$

which by Definition 4 with the input $\tilde{\Delta}$, implies that the error dynamics (25) are zero-output smooth dissipative.

Now, since the system (25) is 0-LUAS, by a converse Lyapunov theorem (e.g., [16]), there exists a C^1 function V_0 for the system (3) such that

$$\alpha_1(e) \leq V_0(e) \leq \alpha_2(e) \tag{31}$$

$$\tfrac{\partial V_0}{\partial t} + \tfrac{\partial V_0}{\partial e} f(t, e, 0) \leq -\alpha_0(\|e\|), \qquad \forall e \in \mathcal{D}_e \tag{32}$$

holds for some continuous positive definite functions α_1, α_2, $\alpha_0 \in \mathcal{K}$. If we take the derivative of V_0 along the trajectories of the whole system (25), we have

$$\tfrac{\partial V_0}{\partial t} + \tfrac{\partial V_0}{\partial e} f(t, e, \tilde{\Delta}) = \tfrac{\partial V_0}{\partial t} + \tfrac{\partial V_0}{\partial e} f(t, e, 0) + \tfrac{\partial V_0}{\partial x}[f(t, e, \tilde{\Delta}) - f(t, e, 0)] \tag{33}$$

Since V_0 is continuously differentiable and we consider e in a compact subset $\mathcal{D}_e$, there exists a positive constant K_{V_0} such that

$$\left\| \frac{\partial V_0}{\partial e} \right\| \leq K_{V_0}, \quad \forall e \in \mathcal{D}_e \tag{34}$$

Moreover, the system (25) is locally Lipschitz in e and $\tilde{\Delta}$, uniformly in t. This implies that there exists a positive constant $L_{\tilde{\Delta}}(e)$ such that

$$\left\| f(t, e, \tilde{\Delta}) - f(t, e, 0) \right\| \leq L_{\tilde{\Delta}}(e)\|\tilde{\Delta}\| \tag{35}$$

$\forall e \in \mathcal{D}_e$, $\forall \tilde{\Delta} \in \mathcal{D}_{\tilde{\Delta}}$, $\forall t \geq 0$. Since $e \in \mathcal{D}_e$, where $\mathcal{D}_e$ is compact, $L_{u_{max}} := \max_{e \in \mathcal{D}_e} L_{\tilde{\Delta}}(e)$ exists. Thus, using the inequality (32), and the definitions for K_{V_0} and $L_{u_{max}}$, we have

$$\tfrac{\partial V_0}{\partial t} + \tfrac{\partial V_0}{\partial e} f(t, e, 0) + \tfrac{\partial V_0}{\partial e}[f(t, e, \tilde{\Delta}) - f(t, e, 0)] \leq -\alpha_0(\|e\|) + K_{V_0} L_{u_{max}} \|\tilde{\Delta}\| \tag{36}$$

After defining the $\mathcal{K}$-function $\sigma_0(s) = K_{V_0} L_{u_{max}} s$, for $s \in \mathbb{R}_{\geq 0}$, we rewrite (36) as

$$\dot{V}_0 \leq -\alpha_0(\|e\|) + \sigma_0(\|\tilde{\Delta}\|) \tag{37}$$

Thus, by Definition 3, V_0 is an iISS Lyapunov function for the system (25). Consider the iISS Lyapunov function V_0 for system (25) satisfying (31) and (37). Then, by sufficiency discussion in [18] and [19], system (25) is locally iISS (LiISS).

Finally, the LiISS property implies that there exist functions $\alpha \in \mathcal{K}$, $\beta \in \mathcal{KL}$ and $\gamma \in \mathcal{K}$, such that, for all $e(0) \in \mathcal{D}_e$ and $\tilde{\Delta} \in \mathcal{D}_{\tilde{\Delta}}$, e is defined and

$$\|e(t)\| \leq \beta(\|e(0)\|, t) + \alpha\Big(\int_0^t \gamma(\|\tilde{\Delta}\|)\Big)ds \tag{38}$$

for all $t \geq 0$. ∎

B. Estimation Module

The motivation behind proving that the system is LiISS with respect to $(\Delta, \dot{\Delta})$ is that, if by an estimation method, the vectors $\|\Delta\|$ and $\|\dot{\Delta}\|$ can be taken to 0, then we can claim via (38) that the system remains stable. The advantage of using this method is that it provides modularity in the sense that the control law can be designed independently from the estimation law [21]. Thus, it would be sufficient to design an estimation law that will take $\|\Delta\|$ and $\|\dot{\Delta}\|$ to 0 over the cycles of motion of the armature. Indeed, electromagnetic actuators are usually used in iterative processes. We will take advantage of this cyclic use of the actuators to estimate the uncertain parameters over cycles. To do so, we propose to use gradient descent-based estimation filters, that will be switched on during the life cycle of the actuator based on a fault detection signal. The fault detection signal that we use is simply based on a cost function measurement, at the final desired motion time t_f, the distance between the desired trajectory z_1^{ref}, z_2^{ref} (refer to Section IV-A) that the armature can track under nominal conditions, and the actual trajectories of the armature. The cost function that we consider here is given by

$$Q = q_1(z_1(t_f) - z_1(t_f)^{ref})^2 + q_2(z_2(t_f) - z_2^{ref}(t_f))^2,\ q_1, q_2 > 0 \tag{39}$$

When the cost function (39) is higher than a predefined fault-threshold, the filters are switched on to estimate the uncertainties that caused the fault, i.e., the tracking performance degradation. The filters start estimating the uncertainties iteratively, in the sense that at each new iteration the filters restart their computations from their new initial conditions given by the final values of the estimated uncertainties obtained at the previous iteration. This iterative estimation process continues until the uncertain parameters are estimated which in turn implies that the cost function drops back below the fault-threshold.

Let us first recall the gradient descent-based filters [21]. We consider the three uncertain parameters $k,\ \eta,\ f_d$. These parameters enter the dynamics through the following equation:

$$\dot{z}_2 = -\frac{a z_3^2}{2m(z_1+b)^2} + \begin{bmatrix} \frac{x_0 - z_1}{m} & \frac{-z_2}{m} & \frac{1}{m} \end{bmatrix}^T \begin{bmatrix} k \\ \eta \\ f_d \end{bmatrix} \tag{40}$$

The main problem with the estimation for the system at hand is that, there is only a single equation through which the uncertain parameters enter the dynamics (40). Due to this model structural constraint, we can estimate only one parameter at a time. Following [21], the filters to estimate each parameter k, η and f_d are given bellow:

- For the parameter k the estimate $\hat{\mathbf{k}}$ is computed as:

$$\begin{aligned}
&\dot{\Omega} = (A_0 - \lambda \tfrac{(x_0-z_1)^2}{m^2} P)\Omega + \tfrac{(x_0-z_1)}{m} \\
&\dot{\Omega}_0 = (A_0 - \lambda \tfrac{(x_0-z_1)^2}{m^2} P)(\Omega_0 + z_2) - \tfrac{\eta z_2}{m} - \tfrac{f_d}{m} + \tfrac{a/2z_3^2}{m(z_1+b)^2} \\
&\epsilon = z_2 + \Omega_0 - \Omega\hat{k} \\
&\dot{\hat{k}} = \Gamma \tfrac{\Omega\epsilon}{1+\nu\Omega^2}.
\end{aligned} \tag{41}$$

- For the parameter η the estimate $\hat{\eta}$ is computed as:

$$\begin{aligned}
&\dot{\Omega} = (A_0 - \lambda \tfrac{z_2^2}{m^2} P)\Omega - \tfrac{z_2}{m} \\
&\dot{\Omega}_0 = (A_0 - \lambda \tfrac{z_2^2}{m^2} P)(\Omega_0 + z_2) - k\tfrac{(x_0-z_1)}{m} - \tfrac{f_d}{m} + \tfrac{a/2z_3^2}{m(z_1+b)^2} \\
&\epsilon = z_2 + \Omega_0 - \Omega\hat{\eta} \\
&\dot{\hat{\eta}} = \Gamma \tfrac{\Omega\epsilon}{1+\nu\Omega^2}.
\end{aligned} \tag{42}$$

Parameter	Value
m	0.27 $[kg]$
R	6 $[\Omega]$
η	7.53 $[kg/sec]$
x_0	8 $[mm]$
k	158 $[N/mm]$
a	14.96×10^{-6} $[Nm^2/A^2]$
b	4×10^{-5} $[m]$

TABLE I: Numerical values of the mechanical parameters

- For the parameter f_d the estimate $\mathbf{\hat{f}_d}$ is computed as:

$$\begin{aligned}
&\dot{\Omega} = (A_0 - \lambda \tfrac{1}{m^2} P)\Omega + \tfrac{1}{m} \\
&\dot{\Omega}_0 = (A_0 - \lambda \tfrac{1}{m^2} P)(\Omega_0 + z_2) - \tfrac{\eta z_2}{m} - k\tfrac{(x_0 - z_1)}{m} + \tfrac{a/2 z_3^2}{m(z_1+b)^2} \\
&\epsilon = z_2 + \Omega_0 - \Omega \hat{f}_d \\
&\dot{\hat{f}}_d = \Gamma \tfrac{\Omega \epsilon}{1+\nu \Omega^2}.
\end{aligned} \tag{43}$$

In the above equation $A_0, P = P^T > 0$ are constant design matrices that satisfy the Lyapunov equation $PA_0 + A_0 P = -I$, and $\lambda > 0$, $\nu > 0$ are design variables.

We can now state the following result.

Lemma 2: Consider the closed-loop dynamics given by (13), (14) and (15), with one constant unknown parameter k, η, or f_d. Then, there exist positive gains c_1, c_2, c_3, κ_1, κ_2 and κ_3 such that the closed-loop dynamics given by (13), (14), (15) and the filters (41), (42), (43) are bounded with asymptotically decreasing tracking errors, and that the unknown parameter is asymptotically estimated.

Proof: The boundedness of the estimation errors Δ, $\dot{\Delta}$ over a finite time interval, together with their asymptotic convergence is known ([21], Lemma 6.5). Next, the boundedness and the asymptotic convergence of the tracking errors e is concluded from the boundedness and convergence of $\tilde{\Delta} = [\Delta, \dot{\Delta}]'$ together with the inequality (38) of Lemma 1. ■

Remark 1: The feedback controller (14) and (15) assumes the knowledge of the state vector z. Cheap, precise and small current sensors are easily available. If the specific application allows it, the armature position can be measured using special sensors, which are usually expensive and bulky, e.g. laser sensors, and the velocity can then be obtained by simple numerical filtering. In some specific applications where it is not possible to incorporate a position sensor, e.g. combustion engines, and artificial heart valves, another solution is to use observers to estimate the armature position and velocity from the current measurements, e.g. using an extension of the Luenberger linear estimator to nonlinear systems presented in [22], or the sliding-mode based observers used in [8].

V. Simulations

We show here the behavior of the proposed approach on the example of electromagnetic actuator presented in [12], where the model (11) is used with the numerical values of Table I. The desired trajectory has been selected as the 5^{th} order polynomial $x^{ref}(t) = \sum_{i=0}^{5} a_i (t/t_f)^i$, where the a_i's have been computed to satisfy the boundary constraints $x^{ref}(0) = 0.2, x^{ref}(t_f) = x_f, \dot{x}^{ref}(0) = \dot{x}^{ref}(t_f) = 0, \ddot{x}^{ref}(0) = \ddot{x}^{ref}(t_f) = 0$, with $t_f = 0.5$ sec, $x_f = 0.7$ mm. To make the simulation tests more realistic we assumed that a random white noise with a maximum excursion of 0.01 mm is added to the position measurement signal. Indeed, in practical settings the armature position could be measured by precise position sensors, e.g. laser sensors, which can generate noisy signals due for example to electrical noises or mechanical vibrations of the armature. We also added a random white noise to the current measurements with an excursion of $2 \times 10^{-6}\ A$. This is a reasonable approximation of the electrical noises in the presently available current sensors, e.g. hall-effect sensors, since these sensors, if properly shielded, have practically very small noise appearing on their output signal. We assumed that the armature velocity is computed from the position signal by direct differentiation. All the measurements are simulated with a sampling rate of $1\ ms$. Furthermore, we imposed saturations on the voltage signal between 0 and 60 volts. Finally, to test the controller performance when dealing with model structural uncertainties, we added in the direct model used in the simulations, the effect of eddy currents on the coil. Following [23], eddy current effect was modelled by adding a R_{eddy}-L_{eddy} circuit in parallel with the coil's electrical circuit. In this case, the model (11) is modified as follows:

$$\begin{aligned} & m\frac{d^2x}{dt^2} = k(x_0 - x) - \eta\frac{dx}{dt} - \frac{ai^2}{2(b+x)^2} + f_d \\ & u = R(i_{eddy} + i) + \frac{a}{b+x}\frac{di}{dt} - \frac{ai}{(b+x)^2}\frac{dx}{dt} \\ & \frac{di_{eddy}}{dt} = \frac{1}{L_{eddy}}(u - R(i + i_{eddy}) - R_{eddy}i_{eddy}) \end{aligned} \tag{44}$$

where, i_{eddy} denotes eddy current. It was shown in [23], via experimental tests, that the model (44) is a good approximation of eddy current effect. We tuned the values of the resistance R_{eddy} and the inductance L_{eddy} to have an eddy current maximum amplitude corresponding to 10% of the coil current i at a nominal functioning of the actuator ($R_{eddy} = 10\ \Omega$, $L_{eddy} = 10\ H$). We also point out here that in this model we do not consider the saturation region of the flux linkage in the magnetic field generated by the coil, since we assume a current and armature motion ranges within the linear region of the flux, which is a reasonable assumption for many applications, e.g. [3], [23]. To test the controller performance we simulate the following scenario: we consider uncertainties in the model appearing sequentially over time. First, at $t = 1\ sec$, we consider that the parameter k has an error $\Delta k = -5\ N/mm$. Next, we consider that at $t = 45\ sec$, the parameter η sustains an error $\Delta\eta = 2\ kg/sec$, finally at $t = 50\ sec$, we assume a disturbance force f_d of $-50N$ (static friction force). We simulate the controller (14) and (15) with the gains $c_1 = 100$, $c_2 = 100$, $c_3 = 2500$, $\kappa_1 = 0.25,\ \kappa_2 = 0.02,\ \kappa_3 = 0.25$. For the filters (41), (42), (43), we use the gains $A_0 = -0.5,\ P = 1,\ \lambda = 1,\ \Gamma = 100$. We underline again here that, due to the structure of the model, we can estimate only one parameter at the time (see Section IV-B). However, in realistic scenarios we do not know which one of these parameters is changing. For this reason, we need to find a way to detect which uncertainty is happening, to do so we propose a simple, yet effective way to detect the type of uncertainty for this particular case of actuators. The general theory of fault detection and identification (FDI) is more complicated (e.g. [24]) and we are not pretending here to propose a new FDI solution for the general case. Indeed, as we mentioned before in Section IV-B, we use the cost function (39) to detect if there is a fault happening in the actuator. After a fault has been detected, we simply swap between the three filters (41), (42) and (43). We apply the first filter (41) for the first iteration after a fault has been detected, and compute the associated cost function value $Q_{\hat{k}}$, then we reset the values of the uncertain parameters to their nominal values and apply the second filter (42) at the second iteration, we then compute the associated cost function $Q_{\hat{\eta}}$. Finally, at the third iteration we reset again all the uncertain parameters to their nominal values and apply the third filter (43), we compute the associated cost value $Q_{\hat{f}d}$. Then we simply compare these three cost values and we select the filter that has the least cost value. The idea behind this logic is that for this particular system we noticed that, if an uncertainty occurred for k then the filter (41) leads the the best cost function and similarly for the two other uncertainties. So even if the faults are not observable directly from the acceleration output because they all enter the acceleration equation in a linear combination, they are still observable via the

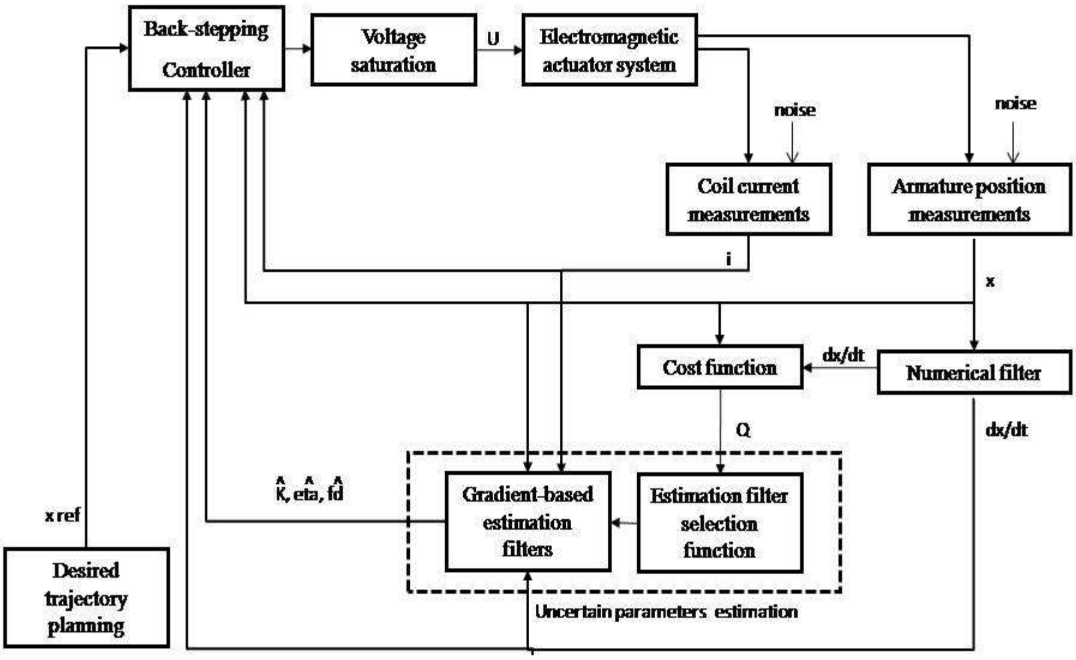

Fig. 1: Feedback control block diagram

cost function output. We now show the efficiency of this simple selection method below. The overall control feedback setting is summarized on the block diagram on figure 1. First, we consider that the uncertainties appear abruptly, i.e., step changes due to a sudden fault in the actuator. We see on figures 2(a), 2(b) and 2(c) that at the instants $1\ sec, 45\ sec$, and $50\ sec$ when the uncertainties occur, the position tracking performances is lost for few iterations (the obtained trajectories in dashed-line start diverging from the desired trajectories in solid-line), but then it is recovered after the fault value has been estimated. This can be seen clearly on figures 2(a) and 2(b) since after the occurrence of the k-fault at $t = 1\ sec$ the position tracking was lost but it was recovered afterwards, as seen on the last iteration just before the occurrence of the η-fault at $t = 45\ sec$. Similar tracking recovery can be observed on figures 2(b) and 2(c) for η and f_d faults. The same loss of performance occurs on the velocity tracking as shown on figures 3(a), 3(b) and 3(c). The associated cost function (39) is plotted in figures 4. The jumps in the cost function due to the occurrence of the first k-uncertainty at $t = 1\ sec$ and the third f_d-fault at $t = 50\ sec$ are clear on figure 4. The other jump at $45\ sec$ due to the η-uncertainty is clear on the zoom shown on figure 4-bottom.

Next, we display on figures 5(a), 5(b), and 5(c), the behavior of the estimation filters. The filters manage to recover the actual value of the uncertainties quickly. The simple logic that we described earlier to automatically identify the current uncertainty and then select the proper filter has shown good performance, since after each fault the selection logic swaps through the different filters and select the best one, as seen for example on figure 5(b), where we see that after the occurrence of the η-uncertainty the value of $\hat{\eta}$ fluctuates while the selection logic is trying the three different filters and quickly the appropriate

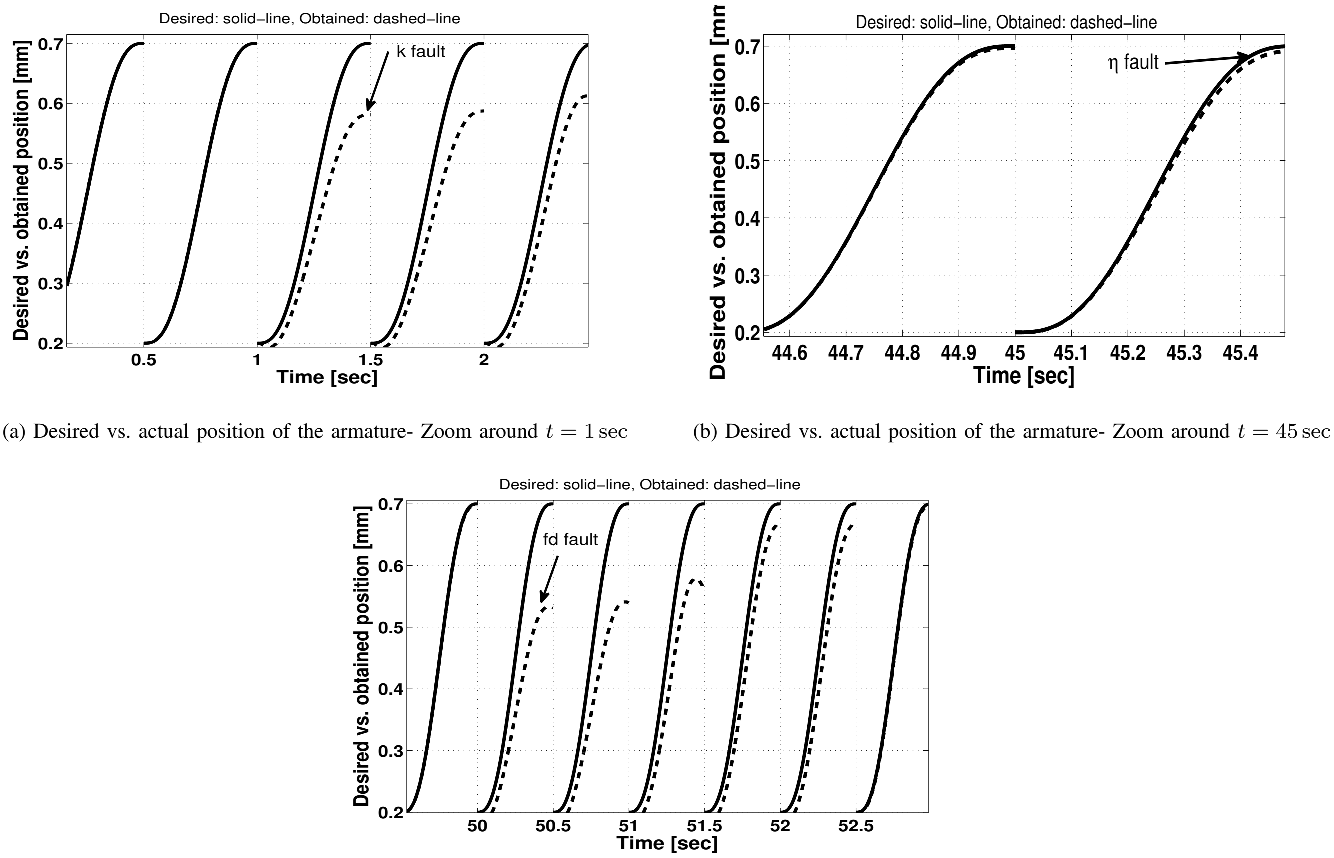

(a) Desired vs. actual position of the armature- Zoom around $t = 1\,\mathrm{sec}$

(b) Desired vs. actual position of the armature- Zoom around $t = 45\,\mathrm{sec}$

(c) Desired vs. actual position of the armature- Zoom around $t = 50\,\mathrm{sec}$

Fig. 2: Desired vs. actual position of the armature

filter, the η-filter in this case, is selected and the estimation of the actual η is achieved within 5 sec of the fault occurrence. Similarly, we see on figure 5(c) that the f_d uncertainty is estimated after few iterations subsequent to the fault occurrence. Finally, we report on figure 6, the control signal during a sample of iterations, to show that the imposed saturation limits are not violated, and that the simulated measurement noise appears on the feedback control signal, but this does not deteriorate the overall performance of the controller.

We also wanted to test the case of time-varying uncertainties, even though, the presented proofs do not explicitly take into account time-varying uncertainties. We tested the following scenario: First, at $t = 1\ sec$, we consider that the spring stiffness k has a time-varying error $\Delta k = -5(1 - exp(-0.5(t-1)))\ [N/mm]$, this error can model the progressive deterioration of the spring. Then, we consider that at $t = 50\ sec$, the parameter η starts drifting following the time function $\Delta\eta = 2(1 - exp(-0.5(t-50)))\ [kg/sec]$. which can model a slowly appearing viscous force. The obtained results are displayed on figures 7, 8(a) and 8(b).

It is clear from figure 7 that the cost function increase, happens gradually in this case, due to the nature of the fault. Furthermore, we see on figures 8(a), 8(b), that the controller is capable of tracking these time-varying uncertainties.

VI. Conclusion

We have studied in this paper the problem of adaptive control for electromagnetic actuators. We have developed a trajectory tracking controller based on an adaptive backstepping approach. The proposed controller uses a modular adaptive design, based on an iISS backstepping controller complemented with a gradient descent-based estimation filters. The controller

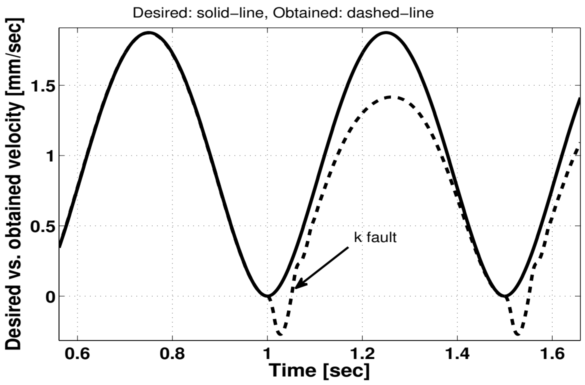

(a) Desired vs. actual velocity of the armature- Zoom around $t = 1\,\mathrm{sec}$

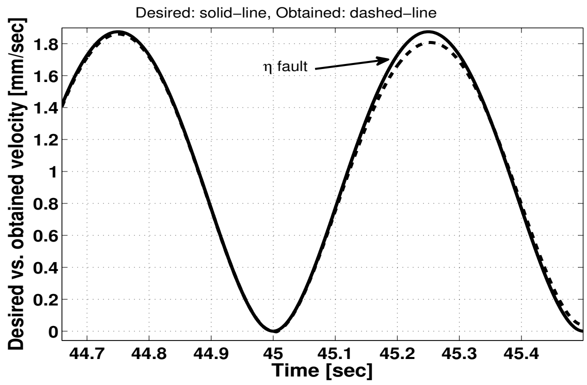

(b) Desired vs. actual velocity of the armature- Zoom around $t = 45\,\mathrm{sec}$

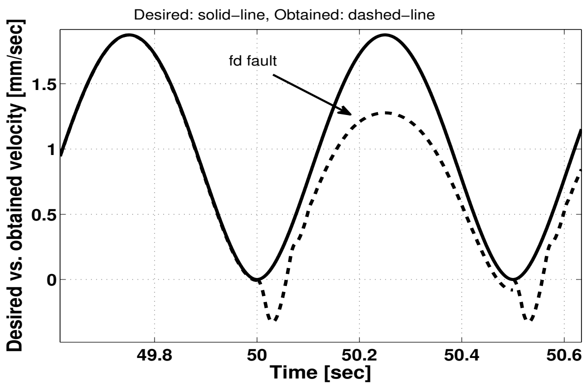

(c) Desired vs. actual velocity of the armature- Zoom around $t = 50\,\mathrm{sec}$

Fig. 3: Desired vs. actual velocity of the armature

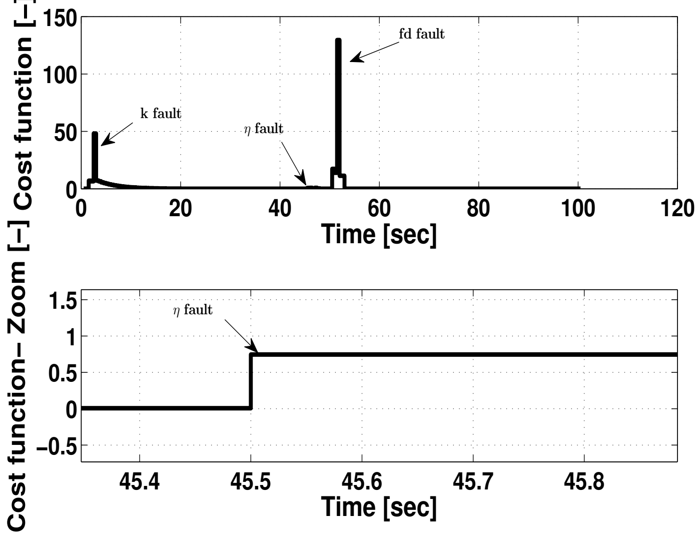

Fig. 4: The cost function (39) with $q_1 = q_2 = 500$

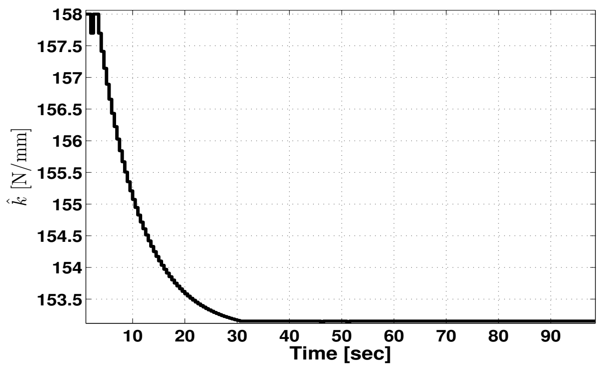

(a) Estimation of k over time

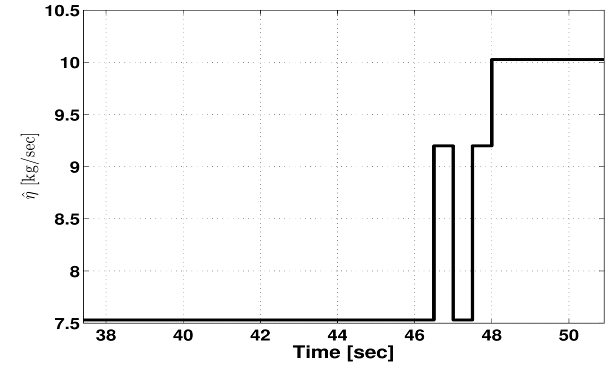

(b) Estimation of η over time- Zoom around $t = 45\,\mathrm{sec}$

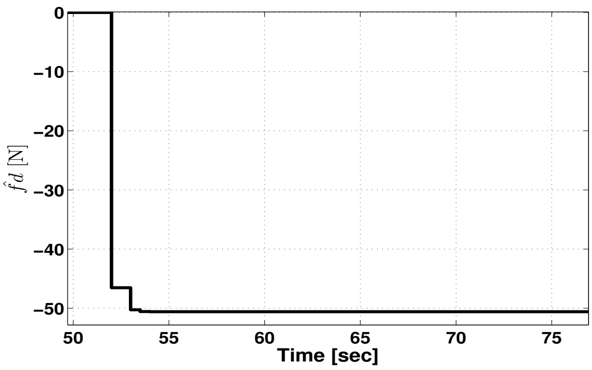

(c) Estimation of f_d over time- Zoom around $t = 50\,\mathrm{sec}$

Fig. 5: Parameters' estimates (time-invariant case)

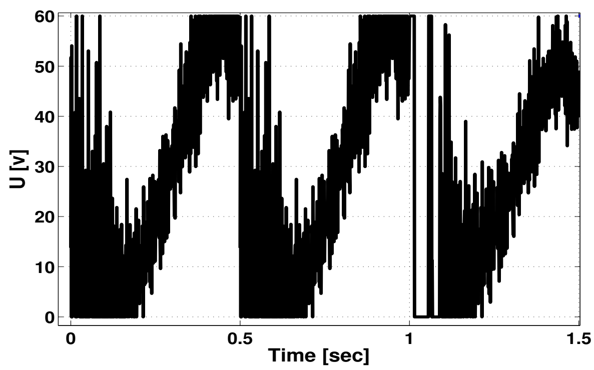

Fig. 6: Zoom on the control voltage

presented here deals with constant uncertainties with linear parametrization. It ensures asymptotic position and velocity tracking error convergence, as well as asymptotic estimation error convergence. We have reported some numerical results showing the performance of the iISS-backstepping adaptive controller. Possible future directions could include extension of the results to explicitly take into account time-varying uncertainties in the control design, as well as uncertainties that appear nonlinearly in model dynamics, e.g. coefficient b of the EMF term. Other possible directions include comparison of model-based approaches with other robust model-free approaches such as extremum seeking [15], in terms of estimation performance, tracking performance and convergence speed.

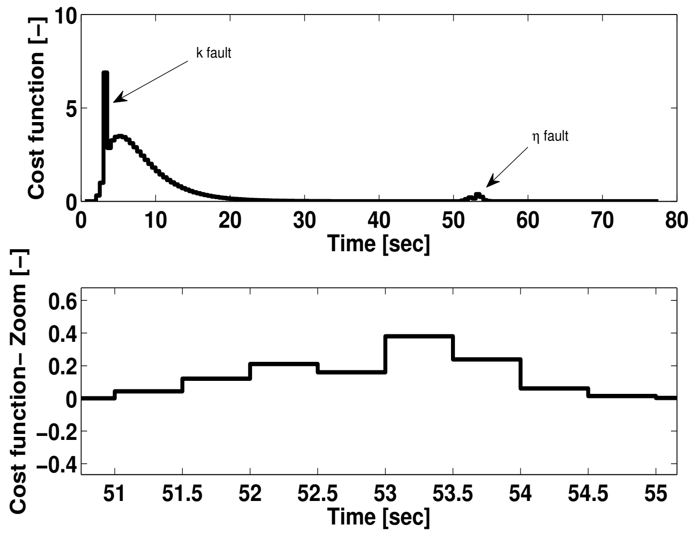

Fig. 7: The cost function (39) with $q_1 = q_2 = 500$

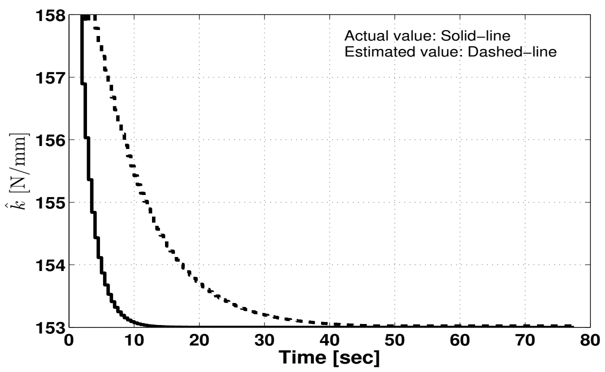

(a) Estimation of k over time

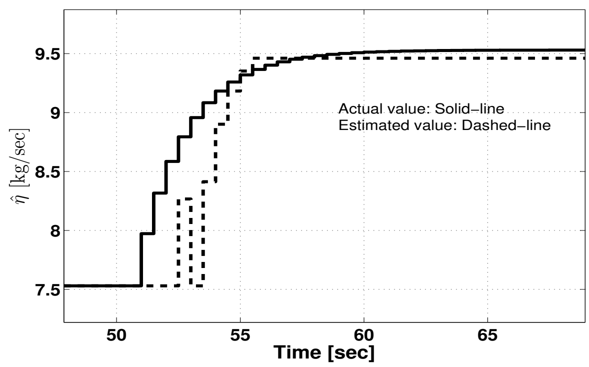

(b) Estimation of η over time

Fig. 8: Parameters' estimates (time-variant case)

REFERENCES

[1] W. Hoffmann, K. Peterson, and A. Stefanopoulou, "Iterative learning control for soft landing of electromechanical valve actuator in camless engines," *IEEE, Transactions on Control Systems Technology*, vol. 11, no. 2, pp. 174–184, March 2003.

[2] J. Tsai, C. Koch, and M. Saif, "Cycle adaptive feedforward approach control of an electromagnetic valve actuator," in *IEEE, Conference on Decision and Control*, Cancun, Mexico, December 2008.

[3] K. Peterson and A. Stefanopoulou, "Extremum seeking control for soft landing of electromechanical valve actuator," *Automatica*, vol. 40, pp. 1063–1069, 2004.

[4] C. Tai and T. Tsao, "Control of an electromechanical camless valve actuator," in *American Control Conference*, May 2002, pp. 262–267.

[5] ——, "Control of an electromechanical camless valve actuator for camless engines," in *American Control Conference*, June 2003, pp. 3113–3118.

[6] K. Peterson and A. Stefanopoulou, "Rendering the electromechanical valve actuator globally asymptotically stable," in *Proceedings of 42nd IEEE Conference on Decision and Control*, Maui, HI, December 2003, pp. 1753–1758.

[7] Y. Wang, A. Stefanopoulou, M. Haghgooie, I. Kolmanovsky, and M. Hammoud, "Modeling of an electromechanical valve actuator for a camless engine," in *Proceedings AVEC*, vol. 5, 2000.

[8] P. Eyabi and G. Washington, "Modeling and sensorless control of an electromagnetic valve actuator," *Mechatronics*, vol. 16, pp. 159–175, 2006.

[9] L. Mianzo and H. Peng, "Output feedback H_∞ preview control of an electro-mechanical valve actuator," *IEEE, Transactions on Control Systems Technology*, vol. 16, 2006.

[10] S. K. Chung, C. R. Koch, and A. F. Lynch, "Flatness-based feedback control of an automotive solenoid valve," *IEEE, Transactions on Control Systems Technology*, vol. 15, no. 2, pp. 394–401, 2007.

[11] Y. Wang, A. Stefanopoulou, M. Haghgooie, I. Kolmanovsky, and M. Hammoud, "Modelling of an electromechanical valve actuator for a camless engine," in *5th International Symposium on Advanced Vehicle Control*, 2000, number 93.

[12] N. Kahveci and I. Kolmanovsky, "Control design for electromagnetic actuators based on backstepping and landing reference governor," in *5th IFAC Symposium on Mechatronic Systems*, Cambridge, September 2010, pp. 393–398.

[13] M. di Bernardo, A. di Gaeta, C. I. . Velasco, and S. Santini, "Energy-based key-on control of a double magnet electromechanical valve actuator," *IEEE, Transactions on Control Systems Technology*, vol. 20, no. 5, pp. 1133–1145, 2012.

[14] M. Benosman and G. Atinc, "Multi-parametric extremum seeking-based learning control for electromagnetic actuators," in *American Control Conference*, 2013, pp. 2643–2648.

[15] ——, "Nonlinear learning-based adaptive control for electromagnetic actuators," in *European Control Conference*, 2013, pp. 2904–2909.

[16] W. Haddad and V. S. Chellaboina, *Nonlinear dynamical systems and control: a Lyapunov-based approach*. Princeton University Press, 2008.

[17] E. Sontag, "Comments on integral variants of iss," *Systems & Control Letters*, vol. 34, no. 1, pp. 93–100, 1998.

[18] H. Ito and Z. Jiang, "Necessary and sufficient small gain conditions for integral input-to-state stable systems: A lyapunov perspective," *IEEE Transactions on Automatic Control*, vol. 54, no. 10, pp. 2389–2404, 2009.

[19] D. Angeli, E. Sontag, and Y. Wang, "A characterization of integral input-to-state stability," *IEEE Transactions on Automatic Control*, vol. 45, no. 6, pp. 1082–1097, 2000.

[20] E. Sontag and Y. Wang, "New characterizations of input-to-state stability," *IEEE Transactions on Automatic Control*, vol. 41, no. 9, pp. 1283–1294, 1996.

[21] M. Krstic, I. Kanellakopoulos, P. Kokotovic, *et al.*, *Nonlinear and adaptive control design*. John Wiley & Sons New York, 1995.

[22] G. Ciccarella, M. D. Mora, and A. Germani, "A luenberger-like observer for nonlinear systems," *Int. Journal of Control*, vol. 57, no. 3, pp. 537–556, 1993.

[23] R. Chladny, C. Koch, and A. Lynch, "Modeling automotive gas-exchange solenoid valve actuators," *IEEE Transactions on Magnetics*, vol. 41, no. 3, March 2005.

[24] M. Benosman, "A survey of some recent results on nonlinear fault tolerant control," *Mathematical Problems in Engineering*, 2010.